

Mapping Repetition Suppression of the N100 Evoked Response to the Human Cerebral Cortex

Nash N. Boutros, Klevest Gjini, Horst Urbach, and Mark E. Pflieger

Background: Repetition suppression (RS) phenomena, such as those observed using paired-identical-stimulus (S1–S2) paradigms, likely reflect adaptive functions such as habituation and, more specifically, sensory gating.

Methods: To better characterize the neural networks underlying RS, we analyzed auditory S1–S2 data from electrodes placed on the cortices of 64 epilepsy patients who were being evaluated for surgical therapy. We identified regions with maximal amplitude responses to S1 (i.e., stimulus registration regions), regions with maximal suppression of responses to S2 relative to S1 (i.e., RS), and regions with no or minimal RS.

Results: Auditory perceptual regions, such as the superior temporal gyri, were shown to have significant initial registration activity (i.e., strong response to S1). Several prefrontal, cingulate, and parietal lobe regions were found to exhibit stronger RS than those recorded from the auditory perceptual areas.

Conclusions: The data strongly suggest that the neural network underlying repetition suppression may include regions not previously thought to be involved, such as the parietal and cingulate cortexes. In addition, the data also support the notion that the initial response to stimuli and the ability to suppress the stimuli if repeated are two separate, but likely related, functions.

Key Words: Cingulate gyrus, frontal lobes, habituation, parietal lobes, temporal lobes, thalamus

The ability to suppress responses to incoming redundant sensory input (i.e., habituation) is a recognized characteristic of the central nervous system (1,2) and has been extensively studied using evoked potential (EP) methodologies (3). In particular, the P50 and N100 midlatency auditory evoked responses (MLAER) have been used to examine habituation using repetition suppression (RS) paradigms. Considerable research has documented that EP habituation is not caused by the effector activity used in most studies to elicit the EP (4), and therefore, intermediate processes such as sensory encoding and stimulus evaluation are hypothesized (5).

Probing N100 RS in neuropsychiatric conditions is promising as evidenced by a growing literature (6–8). More generally, RS has been investigated in a large number of psychiatric and neurological conditions (9) and has proved useful in probing the genetics of neuropsychiatric disorders (10–12).

Average auditory EP responses recorded at the scalp exhibit a sequence of three major components: positive (P50), negative (N100), and positive (P200) deflections (13–15). In RS experiments using the paired-stimulus paradigm (PSP), each MLAER component is suppressed by stimulus repetition. The suppression ratios of the different MLAERs are not correlated (16) and therefore likely are associated with distinct, yet overlapping and interacting, phases of RS. Thus, knowledge about the RS properties of each MLAER component is prerequisite for understanding the entire RS system in the human brain. Although some work has been published regarding

the circuitry underlying P50 gating (17,18), little work addresses the circuitry of N100 gating.

The PSP is widely used to study RS (19,20). When two identical stimuli (S1 and S2) are presented with a short interstimulus interval (ISI), the N100 response to S2 is suppressed. This “N100 suppression” is usually expressed as the S2:S1 ratio of the two N100 responses and is thought to index habituation at the early attentive phases of information processing.

In this study, we adopted an approach for direct functional mapping of N100 RS in the human brain by combining neuroimaging and intracranial electroencephalogram—an opportunity afforded by epilepsy patients who participated in a PSP study while undergoing evaluation as candidates for surgical treatment (21). Specifically, the study aimed to map amplitudes and RS ratios of the N100 using data obtained from grid and strip electrodes placed on various areas of the cortex. We then built on data from current as well as prior work to propose a preliminary model for N100 RS including structures not interrogated in this study, such as the thalamus and hippocampus (3,14).

Methods and Materials

Between 2001 and 2006, 79 patients with drug-resistant focal epilepsies were implanted with cortical electrodes for invasive seizure recordings as part of their presurgical evaluation. All data were collected from the Epilepsy Hospital, Bonn Univeristy, Bonn, Germany. Fifteen subjects were excluded because of extreme artifacts. Data presented here are from the remaining 64 subjects (32 men). Age ranged from 19 to 65 with a mean of 37 ± 12 years.

Patient Characteristics and Clinical Methods

The diagnostic presurgical workup included video-electroencephalogram recordings with surface and subdural/depth electrodes to determine the location of seizure onset, as well as high-resolution magnetic resonance imaging (MRI) (22). Psychiatric status and history were assessed by an experienced psychiatrist (23). All patients were on standard therapy with anticonvulsant drugs.

Electrode placement was verified visually using postimplantation MRI with axial and coronal T2-weighted and fluid-attenuated

From the Department of Psychiatry and Behavioral Neurosciences (NNB, KG), School of Medicine, Wayne State University, Detroit, Michigan; Neuroradiology Department (HU), Bonn University Clinic, Bonn, Germany; and Source Signal Imaging (MEP), San Diego, California.

Address correspondence to Nash Boutros, M.D., Professor of Psychiatry and Neurology, Wayne State University School of Medicine, UPC-Jefferson, 2751 E. Jefferson, Suite 305, Detroit, MI 48207. E-mail: nboutros@med.wayne.edu.

Received Aug 5, 2010; revised Dec 10, 2010; accepted Dec 11, 2010.

inversion recovery sequences (slice thicknesses 2 and 3 mm, respectively) as well as sagittal T1-weighted sequences. Of the 64 subjects, 30 had evidence of pathology on the right hemisphere, 25 on the left hemisphere, and 9 on both sides. Fourteen subjects had pathology localized to one of the medial temporal structures without evidence of neocortical lesions. All patients signed an informed consent approved by both the University of Bonn and Wayne State University.

EP Recording

In a PSP, 75 pairs of identical clicks (S1 and S2; sinusoidal waves, frequency 1500 Hz, Gaussian envelope, duration 4 msec, onset and decay phase of 1.2 msec each) were presented binaurally via headphones with an interstimulus interval of 500 msec and an interpair interval of 8 sec (24). Patients were asked simply to listen to the stimuli. MLAERs were recorded from subdural strip and grid electrodes (sampling rate 1000 Hz per channel, epoch length 1200 msec, prestimulus baseline 200 msec), with reference to both mastoids (bandpass filter setting .03–85 Hz, 12 dB/octave). Details of electrode coverage were published in prior publications (25,26). Figure S1 in Supplement 1 shows all cortical regions where electrodes were placed. Table S1 in Supplement 1 lists all the anatomic regions where electrodes were placed and the number of subjects with electrodes per each region.

All contacts exhibiting N100 responses to S1 were identified by visual inspection, noting the most prominent negative peak in the 70- to 150-msec time window following stimulus onset. A two-step process was employed to increase the confidence that the identified component represents the N100. First, we relied on the well-established scalp morphology of the Vertex Complex (i.e., N100/P200) (27). Components that clearly resembled the N100, as determined by two authors independently, were subjected to the following second step to confirm whether each given channel would be retained for further analysis. Single-trial segments with respect to S1 (–100 to 400 msec) were baseline corrected by subtracting the prestimulus interval (–100 to 0 msec) mean. Then, a paired *t* statistic waveform was obtained by normalizing the mean (across trials) by the standard error (across trials) for each time sample. (This is a paired *t* statistic because each single-trial time-sampled potential is compared against the trial's own baseline, which is identically zero due to prior baseline correction.) Finally, a given channel was confirmed for further analysis (labeled “good”) if the largest negative *t* value in the N100 peaking interval was more negative than the largest negative *t* value in the baseline period; otherwise, the channel was rejected (labeled “bad”) on statistical grounds. Figure S2 in Supplement 1 shows a waveform that was selected visually and confirmed statistically and one chosen visually but rejected statistically. Out of 1065 channels selected visually for all subjects, 271 were rejected, leaving 794 channels for analysis. In total, 107 classified brain regions contained valid data. No other sampled brain regions showed evidence (visual or statistical) of significant N100 activity.

For the S2 response, a similar two-step process was adopted but in a reverse order. Where an S1 was selected, the segmented single-trial S2 responses (–100 to 400 msec) were baseline corrected; *t* statistics were calculated as described for S1; and the largest negative *t* value during the N100 peaking interval was compared with the largest negative *t* value during the baseline period. For S2, the channels were labeled as response present versus response absent. For all channels with response present, N100 S2 components were visually identified. For channels with *t* statistic indicating a nonsignificant difference from baseline, the averages were inspected visually by two investigators to determine whether an S2 component

could confidently be identified based on the morphology of the waveforms. Of the 794 channels over all subjects with confirmed N100 for S1, the S2 N100 was statistically absent for 244. Of these channels, 65 had no visually identifiable N100 and were labeled as having completely attenuated the S2 response (i.e., gating ratio = 0). S2 N100 components were visually identifiable from the remaining 179 channels (over all subjects). All visually identified N100 components were measured from peak to the preceding peak (8). RS was quantified as the $S2/S1 \times 100$ ratio, with higher ratios indicating less effective RS. In patients exhibiting an N100 at several leads within a classified brain region (discussed subsequently), the electrode with the highest N100 amplitude was chosen for determining the degree of RS.

The anatomic regions indicated (Figure S1 in Supplement 1) were used as a guide for pooling the data within closely related anatomic areas. Each designated area had a maximum of three electrodes. From each set of electrodes, the largest (or most significant) value was chosen to represent this area. A number of regions that had more than three electrodes were arbitrarily divided into areas with only three electrodes.

Although negativities occurring around 100 msec poststimulation are detected from the hippocampal region and are likely to be involved in the RS process, we have not classified these as N100 components. Hippocampal results from the same data set have been reported elsewhere (23).

Grids with at least 64 channels (from 20 subjects) were submitted to source analysis. A weighted minimum norm technique (LORETA: low resolution electromagnetic tomography; Curry software implementation) (28) was used to estimate current density distributions for S1 N100 signals and for S1–S2 difference wave potentials. LORETA reconstructs smooth current distributions by assuming that neighboring sources have similar strengths. Individual single-compartment boundary element method (BEM) head models were created from the subjects' MRI data and used to solve the forward problem. Segmentation of the MRI data were performed by an automatic routine of realistic head modeling in Curry software via high resolution discretization of the surfaces with approximately 5000 nodes (about 2000 nodes representing the innermost brain compartment BEM surface). A rotating source type was used instead of fixed source orientations (i.e., cortical surface normals) to allow estimation of omnidirectional currents and to minimize the effects of nonoptimal surface segmentations.

Optimal head modeling for intracranial data are still a matter of research (29). Use of a single-compartment BEM model has been preferred (30), in conjunction with source space spatial smoothing to finesse the issue of whether source depth can be determined reliably from cortical grid recordings (31).

We sought to identify possible functions for those brain regions that were found to contribute to RS. Volumes of interest (VOIs) were defined for each electrode by classifying each gray matter voxel in Montreal Neurological Institute space, as identified using tissue probability map templates, to the nearest electrode position. For functional characterization, we used the BrainMap database (<http://www.brainmap.org>) to identify all experiments that reported at least one focus of activation within each VOI (32). The distribution of behavioral domains and paradigm classes associated with these experiments were then compared with the entirety of the database. The database also includes tasks that were more likely to activate a particular VOI than could be expected if their activations were equally distributed. This in turn allows inference about the functional characteristics of the VOIs (33,34).

Results

Means and standard deviations of N100 amplitudes in the 20 brain regions exhibiting the largest N100 amplitudes are presented in Table S2 in Supplement 1. The recorded N100 components are unlikely to reflect passive volume conduction as contiguous regions showed highly different amplitudes as seen in Figure S3 in Supplement 1.

The largest amplitudes were noted on the dorsal-most part of the right superior temporal gyrus (r-STG) followed by a right parietal region, the dorsal-most part of the middle parietal gyrus (r-MPG). The next five highest amplitudes were recorded from different temporal lobe regions. Thus, five of the six highest amplitude N100 regions were in the STG and MTG (mostly dorsal regions).

Additional regions exhibiting well-formed relatively high-amplitude N100s included one other temporal lobe region, five more parietal lobe areas, four cingulate regions, one occipital lobe area, and two frontal regions. Thus, seven of the 20 highest amplitude regions were parietal and mainly from the inferior parietal gyri. The right and the left midcingulate regions also exhibited well-formed high-amplitude N100s. Included also was the unexpected observation of well-formed N100s on the ventral region of the right inferior occipital gyrus. Finally, two frontal lobe regions also exhibited well-formed relatively high-amplitude N100s (right and left inferior frontal gyri). As can be seen from Figure S3 in Supplement 1, not all regions listed in Table S1 in Supplement 1 show the expected robust grand averages. This reflects increased latency variability in these regions. The calculated means used for Table S1 in Supplement 1 ignore latency variability. It should be noted from Table S1 in Supplement 1 that 7 of the 10 listed highest amplitude regions were from the right hemisphere and only three regions were from the left hemisphere.

Using paired *t* tests to assess the 107 sampled brain regions, the majority (59 regions) exhibited RS, and 38 exhibited no significant RS (10 regions had trends level RS; Table S3 in Supplement 1). The 10 lowest N100 RS ratios (strongest RS) derived from the different brain regions are given in Table S4 in Supplement 1. This table also lists the 10 regions with least RS of the N100 (highest ratios). It should be noted that the RS ratios did not significantly differ among the listed strong RS or among the weak RS regions. The table thus represents a listing of the regions exhibiting most and regions exhibiting least RS. Strongest N100 RS were recorded from electrodes overlaying the ventral right midcingulate area, the ventral region of the left superior parietal gyrus (SPG), the dorsal region of the left superior frontal gyrus (SFG), the middle regions of the left orbitofrontal and right inferior temporal gyrus (r-ITG) regions. Strong, RS was also recorded from the middle area of the left inferior, and the ventral area of the left superior, frontal gyri; the ventral aspect of the left inferior temporal region; the left midcingulate; and the superior ventral region of the right inferior parietal gyrus (r-inferior parietal gyri). Thus, while six of the highest N100 amplitude regions were temporal, only one temporal region (which did not have particularly high amplitude S1) exhibited strong RS. In contrast, four frontal regions exhibited strong RS, whereas there were no frontal regions among the 10 highest amplitude N100 regions. Both the cingulate and parietal regions seem to be involved in both the response to S1 and RS.

Regions with the least RS (Table S4 in Supplement 1; Figure 1) included the lateral-most area of the left orbitofrontal region and the middorsal region of the right frontal pole. It is of interest that among the least gating areas are two regions in close proximity to the area of most gating (i.e., ventral area of the left frontal pole)—

namely, the superior and inferior dorsal regions of the left frontal pole.

Source reconstruction from grid data over the lateral surface of the left hemisphere localized N100 generators for the S1 signal in the STG areas (in five of six grid placements encompassing the left lateral sulcus), in the posterior part of SFG (two of five cases with coverage for that area), and left ventral prefrontal cortex (three of six cases). RS generators from the difference wave (S1–S2) N100 potentials localized to left ventral prefrontal cortex (five of six cases with that area coverage), the posterior part of SFG (two of five cases), and the posterior part of STG (in three of 6 grid placements encompassing the left lateral sulcus; Figure 2: Subject 3, and Figure S4 in Supplement 1).

For subjects with grids placed over the lateral surface of the right hemisphere, N100 generators for the S1 signal were localized in STG areas (in 7 of 7 grid placements encompassing the right lateral sulcus) and in the SPG area (in three of 6 grid placements covering that area), inferior parietal (in five of seven cases), and the posterior part of SFG (two of three cases) cortices. RS generators for N100 S1–S2 difference wave potentials were localized in STG areas (in six of seven cases with respective grid coverage), the SPG area (two of six cases), inferior parietal cortex (in five of seven grid placements), the posterior part of SFG (three of three cases), and the right occipital lobe (one case; Figure 2: Subjects 16 and 18, and Figure S4 in Supplement 1).

Discussion

This study represents a survey of brain regions, monitored for the purpose localizing epileptic lesions, for their initial response to auditory stimuli and the degree of RS. As expected, the temporal cortices exhibited the largest amplitudes N100s (35,36). From the 10 regions exhibiting the largest N100s, 6 were temporal, 2 parietal, and 2 cingulate. Five more parietal regions, two cingulate, two frontal, and one occipital region also exhibited large N100s. These observations suggest that, in addition to the dorsal regions of the STG and MTG, parietal, cingulate, and frontal regions seem also to be involved in the information processing reflected by the N100.

In the data set, four frontal regions exhibited strong RS: dorsal and ventral regions of the left SFG, left orbitofrontal cortex, and the middle region of the left inferior frontal gyri. No frontal regions were among the 10 areas exhibiting largest amplitude N100s. The data thus support a significant role of the frontal lobes in mediating RS (31,37,38). Within the frontal pole area were regions that are within millimeters from each other and yet exhibit strong or minimal RS. Because we now postulate that regions with no RS may also be playing a role in mediating the function, we propose that this functional arrangement is likely of some significance. The frontal pole regions were the only areas where this functional arrangement was detected.

The data also suggest that the parietal and cingulate regions are involved in both stimulus registration (S1) and RS. A number of parietal and cingulate regions exhibited both large N100s and strong RS. This is the first report suggesting the involvement of these regions either in the registration of the stimulus or its RS.

The data strongly suggest that S1 amplitude and RS reflect two distinct functions that are served by different neural circuitries. This assertion is born out from the difference of the topography of the S1 and the S1–S2 difference wave seen in Figure 2 and Figure S4 in Supplement 1. As can be seen from these figures, there is less overlap between the two topographies over the left ventral cortex, the posterior STG, and right occipital cortex. Source reconstruction also showed similar differences between the locations of the gen-

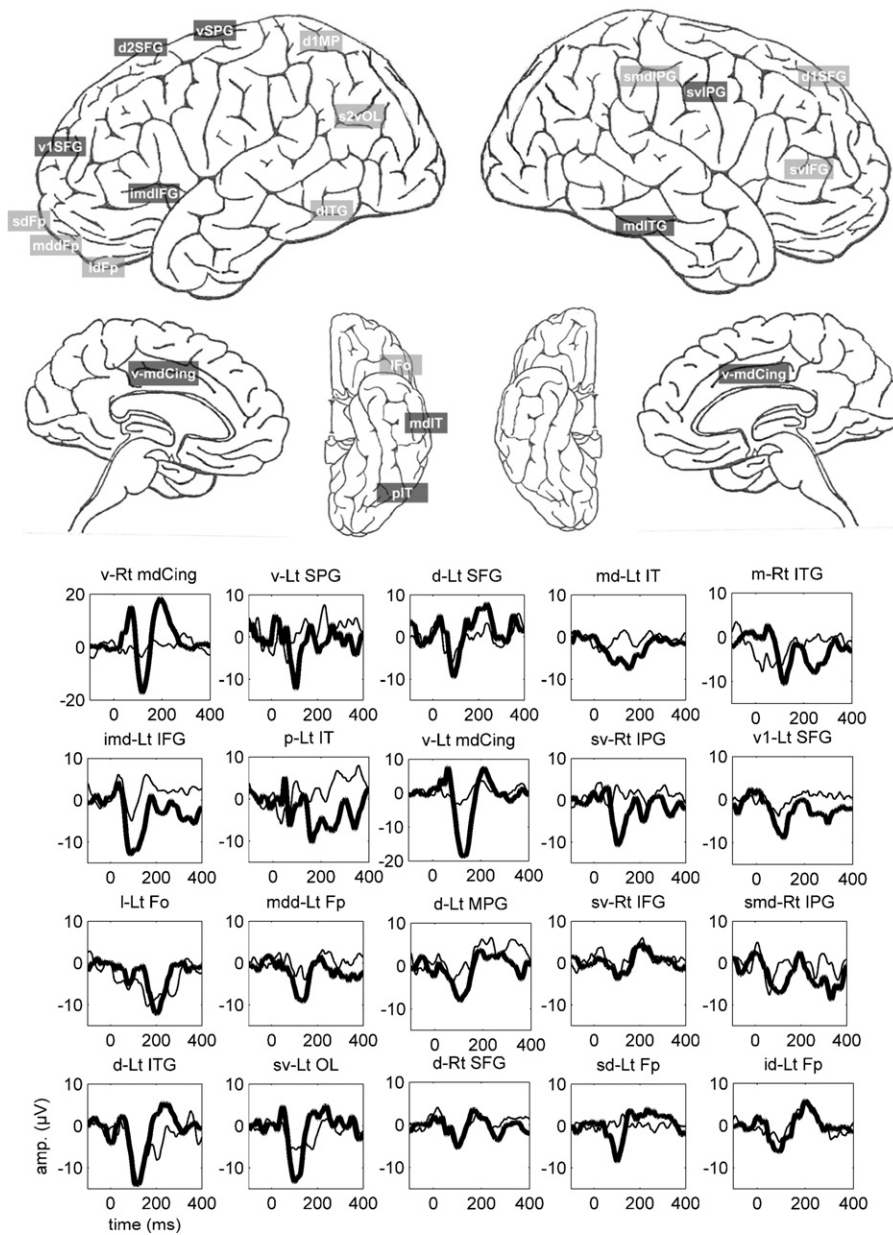


Figure 1. The 10 cortical regions exhibiting maximal gating of the N100 (dark shaded regions), the 10 regions exhibiting the least gating (light shaded areas), and the evoked responses (S1, thick line; S2, thin line) from each region. Lt, left; Rt, right; v-Rt mdCing, ventral mid-cingulate; v-Lt SPG, ventral superior parietal gyrus; d-Lt SFG, dorsal superior frontal gyrus; md-Lt IT, mid-inferior temporal gyrus; md-Rt ITG, mid-inferior temporal gyrus; imd-Lt IFG, inferior mid-inferior frontal gyrus; p-Lt IT, posterior inferior temporal gyrus; v-Lt mdCing, ventral mid-cingulate; sv-Rt IPG, superior ventral inferior parietal gyrus; v1-Lt SFG, ventral superior frontal gyrus; l-Lt Fo, lateral fronto-orbital; mdd-Lt Fp, mid-dorsal frontal pole; d-Lt MPG, dorsal middle parietal gyrus; sv-Rt IFG, superior ventral inferior frontal gyrus; smd-Rt IPG, superior mid-inferior parietal gyrus; d-Lt ITG, dorsal inferior temporal gyrus; sv-Lt OL, superior ventral occipital lobe; d-Rt SFG, dorsal superior frontal gyrus; sd-Lt Fp, superior dorsal frontal pole; id-Lt Fp, inferior dorsal frontal pole.

erators of S1–S2 difference wave and pure S1 N100 potential generators. It should be emphasized that data derived from grid electrodes are limited to the locations of the electrodes and do not fully reflect activity from other brain regions. On the basis of our recent work (39), we believe that the ratio measure (which could not be used for source reconstruction) is more closely linked to S2, whereas the difference measure is more closely related to S1 amplitudes. Hence, we believe that the ratio measure more closely reflects the phenomenon under investigation (i.e., RS). The main purpose of providing the source localization data was to underscore the fact that the two phenomena (i.e., amplitude of S1 and the degree of attenuation of S2) are different functions, possibly mediated by different circuitries. By employing the difference, which (as mentioned) is more closely linked to S1 (40), we may have underestimated the degree of difference between the two functions. Given that the two topographies did not completely overlap in our sample, these data support our hypothesis that the functional anatomy of stimulus registration differs from that of RS.

We also advance the hypothesis that areas exhibiting least RS may be important for the RS functional network, reasoning that some regions must remain responsive for the RS network to evaluate all incoming stimuli. Among the 10 regions exhibiting least RS, 5 were frontal. Only one temporal region exhibited low RS. Regions with almost no RS were mainly on the left side (7 of 10 regions). These observations suggest that although the temporal lobe is paramount for the initial registration of sensory input, it is the frontal lobe (and perhaps the left frontal cortex) that modulates responses to repeating stimuli.

Sable *et al.* (41) provided evidence that N100 RS is not a simple matter of refractoriness but more likely reflects an active inhibitory process. This view was challenged earlier (42) by relating the degree of attenuation to the degree of refractoriness on the basis of the closeness of stimulus repetition. It is important to highlight the fact that although the strongest RS areas were outside the STG, the STG exhibited significant RS from 40% to 60%, which is similar to what is reported in the literature (43).

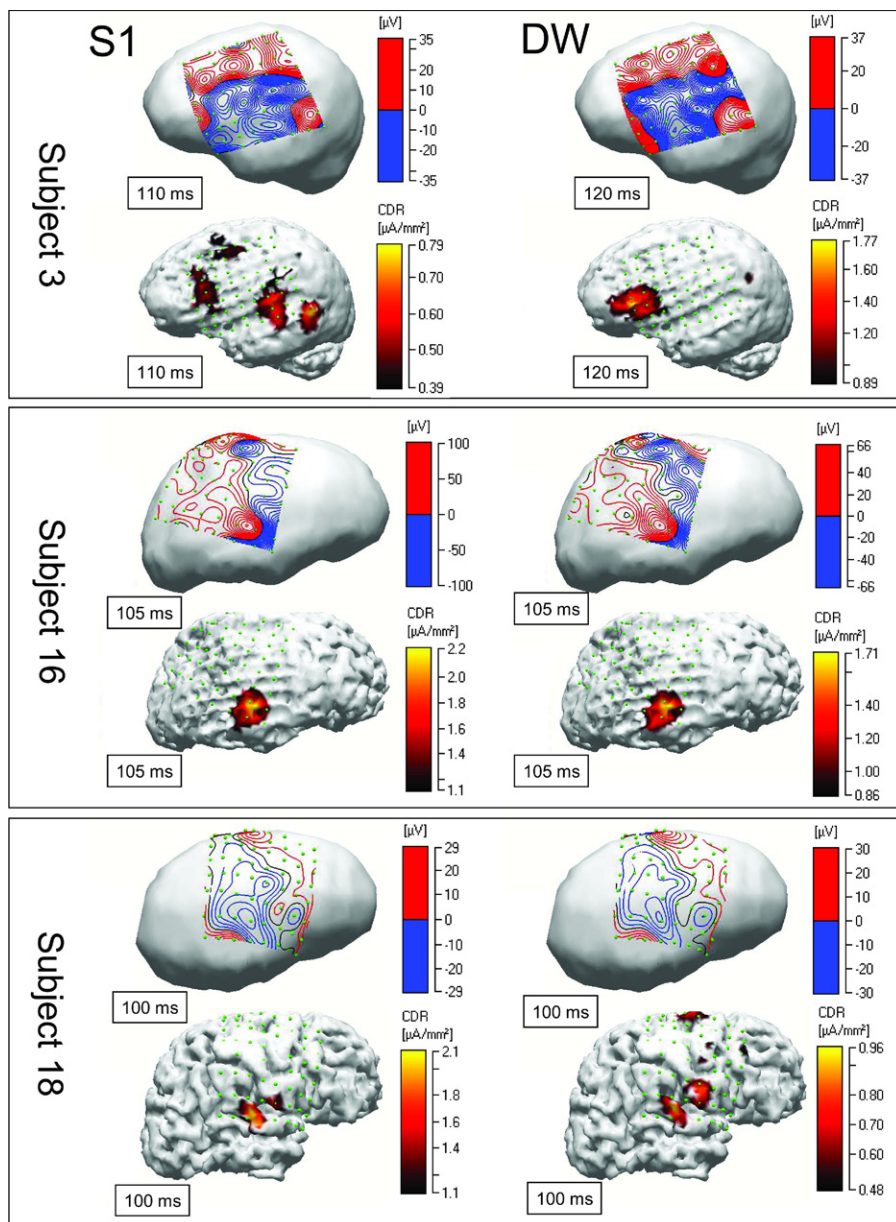


Figure 2. Topographies of the cortical potentials and estimated current densities for 3 (of 20) selected subjects showing differences in cortical potential distributions and generators of S1 signal N100 potential (stimulus registration) and S1–S2 difference waves (sensory gating). Differences are mostly shown in terms of individual regions that are involved in both (Subject 16) or predominantly in one (Subjects 3 and 18) of two processes; stimulus registration and repetition suppression. Data from 20 subjects are shown in Supplement 1. DW, difference wave; CDR, current density reconstruction.

On the basis of correlations between functional studies and the Montreal Neurological Institute idealized MRI, different patterns of functional significance emerge for the strong versus weak RS regions (Table S4 in Supplement 1). Strong RS regions seem to relate mostly to sensory monitoring, whereas weak RS areas are mostly related to cognition. It is thus possible to speculate that both weak and strong RS regions may be playing different roles in mediating the RS function and relating it to subsequent, more elaborate cognitive functioning.

The currently proposed model for P50 RS is centered on the CA3 region of the hippocampus and suggests that the first stimulus (S1) activates both the pyramidal cells and the inhibitory interneurons. Upon arrival of the second stimulus (S2), the still-active inhibitory interneuron prevents or attenuates the response from the pyramidal cells (17,18). This model is too simple, because RS has been shown to be a multistage process (13,44). In addition, a number of regions are involved in RS. Central among these are temporal neocortex and hippocampus, and accumulating evidence strongly

points to the prefrontal cortex as crucial to this function. It is thus possible to consider these three regions as the nuclear auditory RS apparatus. Most prominent among other brain regions that have been implicated in RS is the thalamus, particularly the reticular nucleus (nRT) (45). The involvement of the thalamus was also supported by the observation of worsening somatosensory RS in patients with thalamic strokes (46). Other regions implicated include the amygdala (47,48), proposed to be important in mediating rapid auditory sensory processing involved in emotional conditioning. This study further identifies parietal and cingulate regions as likely contributors, perhaps modulating the nuclear three-site circuit. It is currently not known whether activity in one sensory stream (auditory, visual, or somatosensory) influences RS in other systems. However, the hypothesis that different sensory streams are not completely independent can help to explain the significant involvement of parietal and occipital cortices in the auditory RS paradigm. The foregoing data also implicated the cingulate region. We now postulate that the hippocampal and cingulate regions are engaged in

gating the post-P50 stage of preattentive RS. This is supported by the absence of significant hippocampal activity during the P50 time frame (23,49). Because there is some evidence of frontal activation around the P50 time frame, we postulate that it is involved in the preattentive phase. We also hypothesize a role for the thalamus at the junction between the preattentive (bottom-up) RS process and the early attentive stages (or beginning of a top-down phase) of sensory RS. This role is crucial, because the progression between these two phases is likely to depend on the proper recruitment of the other structures that have been implicated in RS, such as the hippocampus, cingulate cortex, and the amygdala.

It should be acknowledged that using data from individuals with significant brain pathology places serious limitations on the overall interpretation of the results. Although we elected to merge all participants into one group, it is likely that some of the data were influenced by the laterality of the pathology. However, our prior investigation of this possibility did not yield any major findings (50). Also, psychopathology was minimally represented in this group (51). Another limitation of the employed methodology is that the sampling of brain areas is not based on hypotheses by dictated by the clinical situation of the individual subjects. As much as this can be mitigated by the large sample size, there are salient regions that are never sampled using this patient sample, most prominently, the thalamus. Data provided here may help guide future imaging, magnetoencephalography, or dense electrode scalp studies.

This work was supported by the National Institutes of Health (Grant No. RO1 MH063476) and the Joe Young Funds from the Department of Psychiatry and Behavioral Neurosciences, Wayne State University. We thank Dr. Simon Eickhoff of the Department of Psychiatry and Psychotherapy, University of Aachen, Germany, and Dr. Peter Fox from the University of Texas, Health Sciences Center, San Antonio, for their invaluable assistance with relating regions of interest to functional significance.

The authors reported no biomedical financial interests or potential conflicts of interest.

Supplementary material cited in this article is available online.

- Venables P (1964): Input dysfunction in schizophrenia. In: Maher BA, editor. *Progress in Experimental Personality Research*. Orlando, FL: Academic Press, pp 1–47.
- Eisentein EM, Eisenstein D (2006): A behavioral homeostasis theory of habituation and sensitization; further developments and predictions. *Rev Neurosci* 17:533–557.
- Cromwell HC, Mears RP, Wan L, Boutros NN (2008): Sensory gating: A translational effort from basic to clinical science. *Clin EEG Neurosci* 39: 1–4.
- Roemer R, Shagass C, Teyler TJ (1984): Do human evoked potentials habituate? In: Peeke HVS, Petrinovich L, editors. *Habituation, Sensitization and Behavior*. San Diego, CA: Academic Press, 325–346.
- Davis M, Heninger GR (1972): Comparison of response plasticity between the eye-blink and the vertex potential in humans. *Electroencephalogr Clin Neurophysiol* 33:283–293.
- Hsieh MH, Liu K, Liu SK, Chiu MJ, Hwu HG, Chen AC (2004): Memory impairment and auditory evoked potential gating deficit in schizophrenia. *Psychol Res* 130:161–169.
- Brockhaus-Dumke A, Schultze-Lutter F, Mueller R, Tendolkar I, Bechdolf A, Pukrop R (2008): Sensory-gating in schizophrenia: P50 and N100 gating in antipsychotic-free subjects at risk, first-episode and chronic patients. *Biol Psych* 64:376–384.
- Boutros NN, Brockhaus-Dumke A, Gjini K, Vedeniapin A, Elfakhani M, Burroughs S, Keshavan M (2009): Sensory-gating deficit of the N100 mid-latency auditory evoked potential in medicated schizophrenia patients. *Schizophr Res* 113:339–346.
- Patterson JV, Hetrick WP, Boutros NN, Jin Y, Potkin S, Sandman C, Bunney WE Jr (2008): P50 sensory gating ratios in schizophrenics and controls: A review and data analysis. *Psychol Res* 158:226–247.
- Adler LE, Pachtman E, Franks RD, Pecevecich M, Waldo MC, Freedman R (1982): Neurophysiological evidence for a defect in neuronal mechanisms involved in sensory gating in schizophrenia. *Biol Psychiatry* 17: 639–654.
- Siegel C, Waldo M, Mizner G, Adler LE, Freedman R (1984): Deficits in sensory gating in schizophrenic patients and their relatives. Evidence obtained with auditory evoked responses. *Arch Gen Psychiatry* 41:607–612.
- Franks R, Adler L, Waldo M, Alpert J, Freedman R (1983): Neurophysiological studies of sensory gating in mania: Comparison with schizophrenia. *Biol Psychiatry* 18:989–1005.
- Boutros NN, Belger A (1999): Midlatency evoked potentials: Attenuation and augmentation reflect different aspects of sensory gating. *Biol Psychiatry* 45:917–922.
- Grunwald T, Boutros NN, Pezer N, von Oertzen T, Fernandez G, Schaller C, Elger CE (2003): Neural substrates of sensory gating within the human brain. *Biol Psychiatry* 53:511–519.
- Buchsbaum MS (1977): The middle evoked response components and schizophrenia. *Schizophr Bulletin* 3:93–104.
- Boutros NN, Korzyukov O, Jansen B, Feingold A, Bell M (2004a): Sensory-gating deficits during the mid-latency phase of information processing in medicated schizophrenia patients. *Psychol Res* 126:203–215.
- Freedman R, Adler LE, Myles-Worsley M, Nagamoto HT, Miller C, Kisley M, *et al.* (1996): Inhibitory gating of an evoked response to repeated auditory stimuli in schizophrenia and normal subjects. Human recordings, computer simulation, and an animal model. *Arch Gen Psychiatry* 53:1114–1121.
- Moxon KA, Gerhardt GA, Gulinello M, Adler LE (2003): Inhibitory control of sensory gating in a computer model of the CA3 region of the hippocampus. *Biol Cybern* 88:247–264.
- Smith D, Boutros N, Schwarzkopf S (1994): Reliability of P50 auditory event-related potential indices of sensory gating. *Psychophysiology* 31: 495–502.
- Rentzsch J, Jockers-Scherübl MC, Boutros NN, Gallinat J (2008): Test-retest reliability of P50, N100 and P200 auditory SG in healthy subjects. *Int J Psychophysiol* 67:81–90.
- Spencer SS, Sperling MR, Shewmon DA (1997): Intracranial electrodes. In: Engel J, Pedley TA, editors. *Epilepsy: A Comprehensive Textbook*. New York: Lippincott-Raven, 607–612.
- Kral T, Clusmann H, Urbach J, Schramm J, Elger CE, Kurthen M, Grunwald T (2002): Preoperative evaluation for epilepsy surgery Bonn: Algorithm. *Zentralblatt für Neurochirurgie* 63:106–110.
- Boutros NN, Trautner P, Rosburg T, Korzyukov O, Grunwald T, Schaller C, *et al.* (2005): Sensory Gating in the Human hippocampal and rhinal Regions. *Clin Neurophysiol* 116:1967–1974.
- Zouridakis G, Boutros NN (1992): Stimulus parameter effects on the P50 evoked response [Brief report]. *Biol Psychiatry* 32:839–841.
- Kurthen M, Trautner P, Rosburg T, Grunwald T, Dietl T, Kühn KU, *et al.* (2007): Towards a functional topography of sensory gating areas: Invasive P50 recording and electrical stimulation mapping in epilepsy surgery candidates. *Psychiatry Res* 155:121–133.
- Behrens E, Zentner J, van Roost D, Hufnagel A, Elger CE, Schramm J (1994): Subdural and depth electrodes in the presurgical evaluation of epilepsy. *Acta Neurochir* 128:84–87.
- Boutros NN, Korzyukov O, Oliwa G, Feingold A, Campbell D, McClain-Furmanski D, *et al.* (2004b): Morphological and latency abnormalities of the mid-latency auditory evoked responses in schizophrenia: A preliminary report. *Schizophr Res* 70:303–313.
- Pascual-Marqui RD, Michel CM, Lehmann D (1994): Low resolution electromagnetic tomography: A new method for localizing electrical activity in the brain. *Int J Psychophysiol* 18:49–65.
- Acar ZA, Makeig S, Worrell G (2008): Head modeling and cortical source localization in epilepsy. *Conf Proc IEEE Eng Med Biol Soc* 2008:3763–3766.
- Fuchs M, Wagner M, Kastner J (2007): Development of volume conductor and source models to localize epileptic foci. *J Clin Neurophysiol* 24:101–119.
- Korzyukov O, Asano E, Gumenyuk V, Juhász C, Wagner M, Rothermel RD, Chugani HT (2009): Intracranial recording and source localization of auditory brain responses elicited at the 50 ms latency in three children aged from 3 to 16 years. *Brain Topogr* 22:166–175.

32. Eickhoff SB, Laird AR, Grefkes C, Wang LE, Zilles K, Fox PT (2009): Coordinate-based activation likelihood estimation meta-analysis of neuroimaging data: A random-effects approach based on empirical estimates of spatial uncertainty. *Hum Brain Map* 30:2907–2926.
33. Laird AR, Eickhoff SB, Li K, Robin DA, Glahn DC, Fox PT (2009a): Investigating the functional heterogeneity of the default mode network using coordinate-based meta-analytic modeling. *J Neurosci* 29:14496–14505.
34. Laird AR, Eickhoff SB, Kurth F, Fox PM, Uecker AM, Turner JA, *et al.* (2009b): ALE meta-analysis workflows via the brainmap database: Progress towards a probabilistic functional brain atlas. *Front Neuroinformatics* 3:23.
35. Näätänen R, Picton TW (1987): The N1 wave of the human electric and magnetic response to sound. *Psychophysiology* 24:375–425.
36. Giard MH, Perrin F, Echallier JF, Thévenet M, Froment JC, Pernier J (1994): Dissociation of temporal and frontal components in the human auditory N1 wave: A scalp current density and dipole model analysis. *Electroencephalogr Clin Neurophysiol* 92:238–252.
37. Weisser R, Weisbrod M, Roehrig M, Rupp A, Schroeder J, Scherg M (2001): Is frontal lobe involved in the generation of auditory? *Neuroreport* 12:3303–3307.
38. Weiland BJ, Boutros NN, Moran JM, Tepley N, Bowyer SM (2008): Evidence for a frontal cortex role in mediating both auditory and somatosensory habituation: A MEG study. *Neuroimage* 42:827–835.
39. Fuerst DR, Gallinat J, Boutros NN (2007): Range of sensory gating values and test-retest reliability in normal subjects. *Psychophysiology* 44:620–626.
40. Atchley WR, Gaskins CT, Anderson D (1976): Statistical properties of ratios. I. Empirical results. *System Zool* 25:127–148.
41. Sable JJ, Low KA, Maclin EL, Fabiani M, Gratton G (2004): Latent inhibition mediates N1 attenuation to repeating sounds. *Psychophysiology* 41:636–642.
42. Budd TW, Barry RJ, Gordon E, Rennie C, Michie PT (1998): Decrement of the N1 auditory event-related potential with stimulus repetition: Habituation vs. refractoriness. *Int J Psychophys* 31:51–86.
43. Hanlon FM, Miller GA, Thoma RJ, Irwin J, Jones A, Moses SM, *et al.* (2005): Distinct M50 and M100 auditory gating deficits in schizophrenia. *Psychophysiology* 42:417–427.
44. Gjini K, Arfken C, Boutros NN (2010): Relationships between sensory “gating out” and sensory “gating in” of auditory evoked potentials in schizophrenia: Preliminary results. *Schizophr Res* 121:139–145.
45. Krause M, Hoffmann WE, Hajos M (2003): Auditory sensory gating in hippocampus and reticular thalamic neurons in anesthetized rats. *Biol Psychiatry* 53:244–253.
46. Stains WR, Black SE, Graham SJ, McIlroy WE (2002): Somatosensory gating and recovery from stroke involving the thalamus. *Stroke* 33:2642–2651.
47. Cromwell HC, Anstrom K, Azarov A, Woodward DJ (2005): Auditory inhibitory gating in the amygdale: Single-unit analysis in the behaving rat. *Brain Res* 1043:12–23.
48. Cromwell HC, Woodward DJ (2007): Inhibitory gating of single unit activity in the amygdale: Effects of ketamine, haloperidol, or nicotine. *Biol Psychiatry* 61:880–889.
49. Boutros NN, Mears R, Pflieger PE, Moxon KA, Ludowig E, Rosburg T (2008): Sensory gating in the human hippocampal and rhinal regions: Regional differences. *Hippocampus* 18:310–316.
50. Rosburg T, Trautner P, Ludowig E, Helmstaedter C, Bien CG, Elger CE, Boutros NN (2008): Sensory gating in epilepsy-effects of lateralization of hippocampal sclerosis. *Clin Neurophysiol* 119:1310–1319.
51. Boutros NN, Trautner P, Rosburg T, Korzyukov O, Grunwald T, Schaller C, *et al.* (2006): Mid-latency auditory evoked responses and sensory gating in focal epilepsy. *J Neuropsychiatry Clin Neurosci* 18:409–416.